Chemosphere 283 (2021) 131155

Contents lists available at ScienceDirect

Chemosphere

journal homepage: www.elsevier.com/locate/chemosphere

Selective interaction of microcystin congeners with zebrafish (*Danio rerio*) Oatp1d1 transporter

Petra Marić [a,1], Marijan Ahel [b], Nikola Maraković [c], Jovica Lončar [a], Ivan Mihaljević [a], Tvrtko Smital [a,*]

[a] Laboratory for Molecular Ecotoxicology, Division for Marine and Environmental Research, Ruđer Bošković Institute, Bijenička 54, Zagreb, Croatia
[b] Laboratory for Analytical Chemistry and Biogeochemistry of Organic Compounds, Division for Marine and Environmental Research, Ruđer Bošković Institute, Bijenička 54, 10000, Zagreb, Croatia
[c] Institute for Medical Research and Occupational Health, Ksaverska Cesta 2, 10000, Zagreb, Croatia

ARTICLE INFO

Handling Editor: James Lazorchak

Kewwords:
Microcystins
Zebrafish Oatp1d1
Kinetics determinations
Substrates vs. inhibitors
Chemicaly analytical determinations
Molecular docking

ABSTRACT

Microcystins (MCs) are the most studied cyanotoxins. The uptake of MCs in cells and tissues of mammals and fish species is mostly mediated by organic anion-transporting polypeptides (OATPs in humans and rodents; Oatps in other species), and the Oatp1d1 appears to be a major transporter for MCs in fish. In this study, six MC congeners of varying physicochemical properties (MC-LR, -RR, -YR, -LW, -LF, -LA) were tested by measuring their effect on the uptake of model Oatp1d1 fluorescent substrate Lucifer yellow (LY) in HEK293T cells transiently or stably overexpressing zebrafish Oatp1d1. MC-LW and -LF showed the strongest interaction resulting in an almost complete inhibition of LY transport with IC_{50} values of 0.21 and 0.26 μM, while congeners -LR, -YR and -LA showed lower inhibitory effects. To discern between Oatp1d1 substrates and inhibitors, results were complemented by Michaelis–Menten kinetics and chemical analytical determinations of MCs uptake, along with molecular docking studies performed using the developed zebrafish Oatp1d1 homology model. Our study showed that Oatp1d1-mediated transport of MCs could be largely dependent on their basic physicochemical properties, with log P_{OW} being the most obvious determinant. Finally, apart from determination of the chemical composition of cynobacterial blooms, a reliable risk assessment should take into account the interaction of identified MC congeners with Oatp1d1 as their primary transporter, and herewith we demonstrated that such a comprehensive approach could be based on the use of highly specific *in vitro* models, accompanied by chemical assessment and *in silico* molecular docking studies.

1. Introduction

Cyanobacteria are marine, freshwater or terrestrial photosynthetic bacteria that possess the ability to produce a wide variety of secondary metabolites which enable them to modify their habitats and thrive under diverse environmental stress conditions (Sivonen and Jones, 1999; Dittmann et al., 2013). Cyanobacterial secondary metabolites are in most cases highly bioactive substances, and some of them, called cyanotoxins, have been shown to present a significant risk to livestock, fish, other aquatic organisms and human health upon their release into aquatic environments during so-called harmful algal blooms (HABs). HABs are a phenomenon that typically occurs in aquatic ecosystems in conditions of high nutrient input, eutrophication and increased temperature. They can be formed by various genera of cyanotoxin-producing cyanobacteria (toxic strains) and non-cyanotoxin-producing cyanobacteria (non-toxic strains) (D'Anglada at al., 2016; Zohdi and Abbaspour, 2019).

Considering the increased occurrence of cyanobacterial blooms, as well as human and animal poisonings (Wang et al., 2021), much effort has been put into revealing the toxic effects and molecular mechanisms

Abbreviations: MC, microcystin; OATP/Oatp, organic anion-transporting polypeptide; HAB, harmful algal bloom; LY, Lucifer yellow; HEK293T, human embryonic kidney cells; LC-MS, liquid chromatography-mass spectrometry; QTOF-MS, quadrupole-time-of-flight/mass spectrometry; TIC, total ion current; UPLC, ultra-performance liquid chromatography.

* Corresponding author. Division for Marine and Environmental Research, Ruđer Bošković Institute, Bijenicka 54, 10 000, Zagreb, Croatia.
E-mail address: smital@irb.hr (T. Smital).
[1] Present address: Early Environmental Safety, Crop Science, Bayer AG, Alfred-Nobel-Straße 50, 40789 Monheim am Rhein, Germany.

https://doi.org/10.1016/j.chemosphere.2021.131155
Received 23 February 2021; Received in revised form 6 June 2021; Accepted 8 June 2021
Available online 10 June 2021

of cyanobacterial toxicity (reviewed e.g., in Ferrão-Filho and Kozlowsky-Suzuki, 2011; Buratti et al., 2017). Among the many types of cyanotoxins, microcystins (MCs) are the most dominant in cyanobacterial blooms. They have been shown to be highly toxic and they are often associated with hepatotoxicity, nephropathy, neurotoxicity and other severe toxic effects, particularly upon harmful algal blooms (Chen et al., 2009). MCs are highly diverse in terms of molecular size, structure and physicochemical properties, with almost 280 congeners identified so far (Bouaïcha et al., 2019). A typical MC structure consists of seven amino acids in a ring formation (cyclic heptapeptides) with an obligatory presence of a β-amino acid side chain (ADDA group), and their nomenclature is primarily based on two variable amino acids that are always occupied by L-amino acids (Fig. S1 in Supplementary Material).

The mechanisms of toxicity related to MCs are diverse, and the most studied one includes interactions with protein phosphatases PP1 and PP2A which in turn lead to the hyperphosphorylation of cellular proteins, DNA destruction, inflammation, apoptosis, hepatic hemorrhage and necrosis (MacKintosh et al., 1990). Induction of oxidative stress and interaction with cellular uptake mechanisms is also associated with exposure to MCs, causing cytoskeletal disruption, cancer cell invasion and DNA damage (reviewed e.g., in McLellan and Manderville, 2017; Bouaïcha et al., 2019). As shown in several studies, the toxic potential of MCs depends on their toxicodynamics and toxicokinetics properties, and along with their inhibitory potency towards serine/threonine protein phosphatases (PPs), their uptake kinetics is probably a key determinative of the organ and/or species-specific toxicity of individual congeners. Interaction of MCs with serine/threonine PPs has been extensively addressed in numerous studies and data show that most toxic congeners frequently found in HABs have similar potency in the inhibition of PP1, PP2, and PP4-6, typically showing IC_{50} values in the range of 0.1–1 nM (Bouaïcha et al., 2019). The inhibition of the PPs activity by MCs results primarily from non-covalent interactions, although covalent interaction does occur between MCs and the catalytic sub-units of PPs. However, formation of the covalent bond occurs slowly, and is not essential for the inactivation of the PPs by MCs (Craig et al., 1996; Hastie et al., 2005; Pereira et al., 2011).

Considering the uptake of MCs in various cells and tissues of mammals and fish species, it is mostly mediated by organic anion-transporting polypeptides (OATPs in humans and rodents; Oatps in fish and other species) (Fischer et al., 2010; Niedermeyer et al., 2014; Steiner et al., 2015). OATPs/Oatps are transmembrane proteins that typically consist of 12 transmembrane domains, and their primary physiological role appears to be the hepatic transport of steroid and thyroid hormones, bile salts, prostaglandins and oligopeptides. However, they have been shown to be involved in the transport of endo- and xenobiotics. They are typically polyspecific and expressed in most tissues, with specific members dominantly expressed in toxicologically important organs as the liver or kidney (Hagenbuch and Meier, 2003; Popovic et al., 2010). Transport of MCs has been demonstrated for human OATP1B1 and OATP1B3, and rat and mice OATP1B2 (Fischer et al., 2005; Komatsu et al., 2007). Members of the Oatp1 family were shown to interact with MCs in fish species such as the little skate, rainbow trout and zebrafish. Considering tissue distribution of Oatp1 transcripts, the level of their expression, and specificity towards MC congeners, the Oatp1d1 appears to be dominant transporter of MCs (Meier-Abt et al., 2007; Bury et al., 1998; Bieczynski et al., 2014; Steiner et al., 2015; Faltermann et al., 2016).

From the ecotoxicological perspective, it is important to emphasize that the studies done so far indicate that the rate of MCs uptake, determined e.g., in zebrafish as a cyprinid fish model, varies for different congeners which may partially explain the observed differences in their toxic potential. Furthermore, as Oatp1d1 transporter appears to be highly relevant for uptake of MCs in zebrafish, it is important to better understand the potency and type of interaction of structurally and chemically different MC congeners with fish Oapt1d1. If the interaction of various MCs with Oatp1d1 is significantly different, both in terms of their potency and type of interaction, the presence of highly toxic congeners in HABs might not represent high ecological risk if their Oatp1d1 transport is low. On the contrary, the presence of less toxic congeners with high rate of Oatp1d1 mediated transport could be highly deleterious. Therefore, in this study we addressed this topic using a zebrafish model: six MC congeners of varying physicochemical properties (MC-LR, -RR, -YR, -LW, -LF, -LA) that are frequently found in HABs were tested for their interaction with a target transporter using HEK 293T cells transiently or stably expressing zebrafish Oatp1d1 cloned from zebrafish liver. Results of interaction studies were further verified by chemical analytical determinations of MC uptake in transfected cells, and by molecular docking studies performed for specific congeners.

2. Materials and methods

2.1. Chemicals

Model fluorescent substrate Lucifer yellow (LY), Trypsin-EDTA solution and Hepes were purchased from Sigma-Aldrich, St. Louis, MO, USA. Dulbecco's Modified Eagle's Medium (DMEM) (Powder, High Glucose, Pyruvate), Fetal Bovine Serum (FBS) and Phosphate Buffer Saline (PBS) were purchased from Gibco Invitrogen, Life technologies, CA, USA. The other solvents and salts used were of the highest analytical grade and purchased from Kemika, Zagreb, Croatia.

2.2. Microcystins standards

Six microcystin (MC) congeners were purchased from Enzo Life Sciences: MC-LR, -RR, -YR, -LW, -LF, and -LA. Stock standard solutions were prepared in methanol and stored at −80 °C. Concentrations of stock standard solutions made for analytical LC-MS analyses were 1 μg/μL, while the stock concentrations used for bioassays were 10 mM (-LR) and 1 mM (-RR, -YR, -LW, -LF, and -LA). For LC-MS analyses, stock standards were diluted 1/100 in methanol (final concentrations 10 ng/μL). An overview of the structure and basic chemical and physical properties of microcystin congeners tested in this study has been provided in the Supplementary Material (Table S1; Fig. S1).

2.3. Oatp1d1 transport activity measurements

Interaction of selected MCs with zebrafish Oatp1d1 transporter was determined by using the uptake transport assay with transiently transfected human embryonic kidney HEK239T cells overexpressing the Oatp1d1 uptake transporter cloned from zebrafish liver, as described previously (Popovic et al., 2013; Marić et al., 2017). Briefly, HEK293T cells overexpressing zebrafish Oatp1d1 were co-exposed for 5 min to serial dilutions of MCs and LY as a model substrate, and the rate of Oatp1d1 LY transport was determined. MCs were tested in the concentration range from 0.02 to 100 μM, the final concentration of Oatp1d1-specific substrate LY used in the assays was 10 μM, and the maximal amount of solvents (MeOH for MCs, dimethyl sulfoxide (DMSO) for LY) never exceeded 0.1%. After incubation, the cells were washed twice with an ice-cold incubation medium (250 μL/well) and incubated with 250 μL/well of 0.1% sodium dodecyl sulfate (SDS) for 30 min at 37 °C for cell lysis. Fluorescence of transport specific substrates was measured in 96-well black microplates using a microplate reader (Infinite M200, Tecan, Salzburg, Austria) at specific wavelengths of 425/540 nm. The eukaryotic vector pcDNA3.1(+)/His without cloned genes (mock-transfected cells) was also transfected into the HEK293T cells in order to determine non-transporter specific uptake. Oatp1d1-transfected cells exposed only to incubation medium were used as an additional negative control.

2.4. Type of interaction of MCs with Oatp1d1 transporter

2.4.1. Michaelis-Menten transport kinetics

Stable expression of zebrafish Oatp1d1 in genetically engineered HEK293 Flp-In cells (Thermo Fisher Scientific, Waltham, USA) was achieved using a non-clonal selection, by targeted integration of the *oatp1d1* sequence subcloned into integration vector pcDNA5/FRT (Thermo Fisher Scientific, Waltham, USA) with combination of restriction enzymes HindIII/XhoI. pcDNA5/FRT/Oatp1d1 constructs were specifically targeted into the genome of the Flp-InTM-293 cells following the manufacturer's instructions, using basically the same protocol as described in Lončar and Smital (2018). Zebrafish Oatp1d1 stable transfectants were functionally verified by determination of the uptake rate of model fluorescent substrate LY in comparison to mock-transfected cells, and the stable cell line was further maintained in the same conditions as regular HEK293T cells.

For the type of interaction experiments, HEK293T Flip-In/Oatp1d1 cells were seeded in 96-well plates at a density of 5 or 8 $\times$ 10^5 cells/

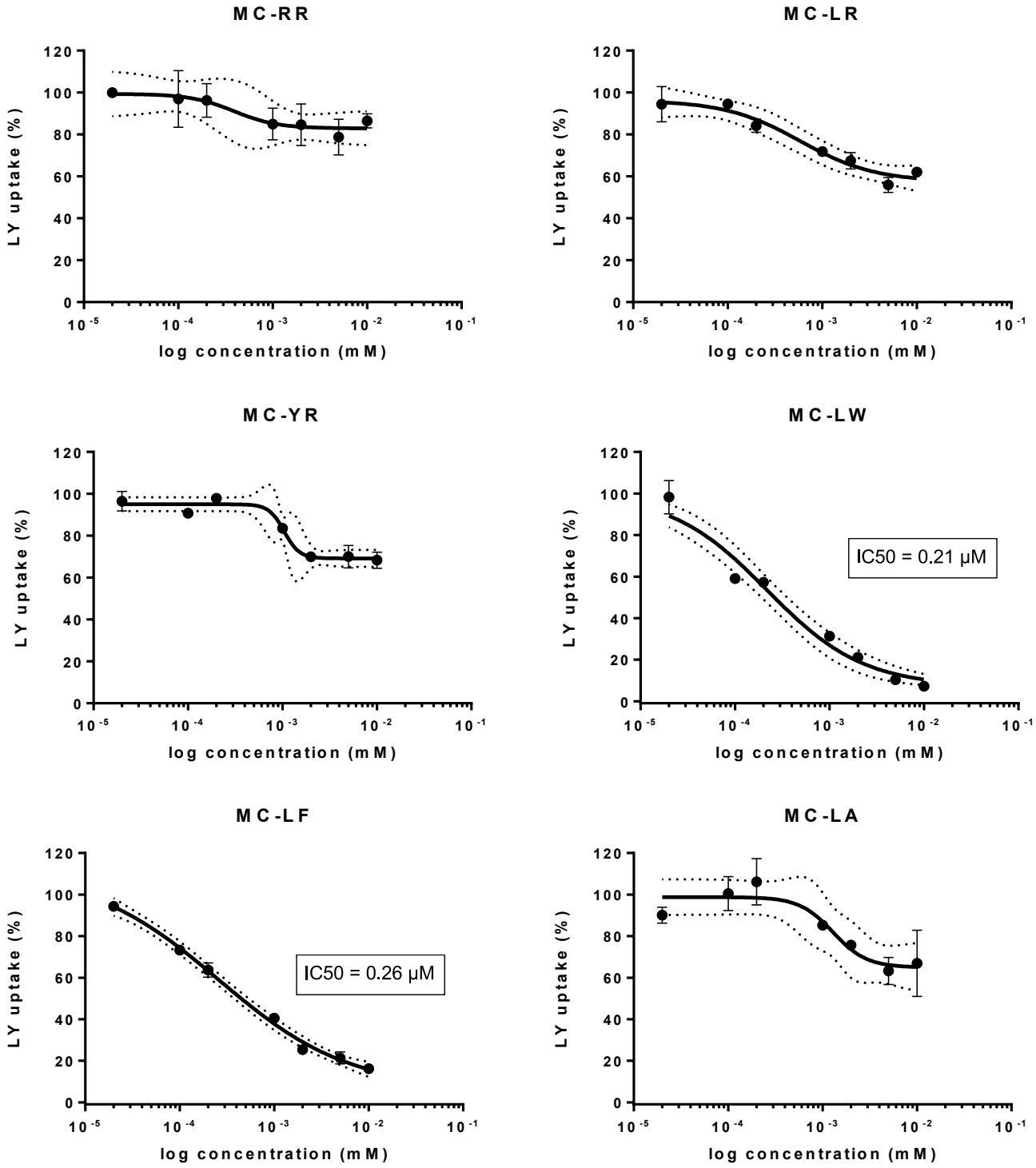

Fig. 1. Concentration-dependent inhibition of zebrafish Oatp1d1 transport activity by MC congeners -RR, -LR, - YR, -LW, -LF and -LA. Results from a typical experiment are shown as percentages of LY uptake in HEK293 FlpIn/Oatp1d1 cells. Each data point represents the mean ± SD from a typical experiment out of three independent determinations. Dotted lines represent 95% confidence intervals.

mL in a final volume of 125 μL/well. Forty-eight hours after seeding, the growth medium was extracted from the cells and 100 μL/well of incubation medium (145 mM NaCl, 3 mM KCl, 1 mM $CaCl_2$, 0.5 mM $MgCl_2$, 5 mM D-glucose, and 5 mM HEPES) was added. Preincubation lasted for 10 min after which 25 μL/well of medium was removed. The activity of the Oatp1d1 transporter was measured by exposing the cells to six concentrations of model substrate LY (5–300 μM) and two to three concentrations of MCs as determined based on results of initial concentration response experiments (Fig. 1): 1 and 10 μM for LC-YR and -LA; 10 and 100 μM for -LR; and for -LW and -LF congeners the concentrations that resulted in 30, 50 and 70% inhibition of LY uptake, respectively, were applied. The exposure volume of LY and MCs added to the cells was 25 μL/well. The maximal amount of DMSO and MeOH used as solvents in all of the tested samples never exceeded 0.1%. A shift in the K_m and V_{max} values of Oatp1d1 transport was determined after 15 min incubation of LY with MCs, as the uptake of LY is linear during the first 15 min of incubation (Fig. S5). After incubation, the cells were washed twice with 125 μL/well of cold incubation medium and subsequently incubated with 125 μL/well of 0.1% SDS for 30 min at 37 °C for cell lysis. As a control, the activity of the Oatp1d1 transporter in HEK293T Flip-In/Oatp1d1 cells was measured in the presence of model substrate LY only (six concentrations). The uptake into HEK293T Flip-In/mock cells was subtracted to obtain transporter-specific uptake. The K_m increase and no changes in V_{max} indicated MCs as substrates (competitive inhibition); no significant changes in K_m and reduced V_{max} pointed to non-competitive inhibition; and reduced K_m and V_{max} indicated un-competitive inhibition. The measurements were done in duplicates and conducted in two to three independent experiments, and results of representative experiments are shown in the Results section. To obtain a linear calibration curve, the fluorescent dye LY was dissolved in 0.1% SDS, in the cell matrix dissolved in 0.1% SDS and in the incubation medium to obtain the linear calibration curves. Bradford assay was used to measure total protein concentration (Bradford, 1976). Based on total protein measurements and the obtained linear calibration curves, the uptake rate of LY was calculated and expressed as nmol of substrate per μg of protein per minute.

2.4.2. Chemical analytical verification of the type of interaction

The MCs that showed significant interaction with zebrafish Oatp1d1 were preliminarily classified as substrates (competitive inhibitors) or non/un-competitive inhibitors based on results of Michaelis-Menten kinetics experiments. They were then further verified on the type of interaction by exposure of HEK293T Flip-In/Oatp1d1 stable transfectants and mock-transfected cells to MCs followed by a chemical analytical determination of the intracellular accumulation of the tested MCs by LC-MS analyses. Cells were seeded in 24-well plates at 8×10^5 cells/mL density in a final volume of 500 μL/well and 48 h after seeding were exposed to different concentrations of MCs. After removing the growth medium above the cells, preincubation was initiated by adding 400 μL/well of incubation medium. Ten minutes later, HEK293T Flip-In/Oatp1d1 cells were exposed to three MC concentrations selected based on the initial transport activity determinations: 0.1, 0.5 and 1 μM for MC-LW and -LF; 0.5, 1 and 5 μM for MC-LA and -YR; 5, 20 and 50 μM for MC-LR. The maximal amount of MeOH used as solvent in all of the tested samples never exceeded 0.5%. Incubation with MCs lasted for 30 min after which cells were washed two times with 500 μL/well of incubation medium. The cells were then incubated in 500 μL/well of MeOH for 30 min at 37 °C in order to permeabilize the cells and extract the accumulated MCs. HEK293T Flip-In/mock cells were also exposed to *the same concentrations of MCs in order to discern between transporter-specific and passive uptake of* the tested MCs. After the final incubation in MeOH, cells were manually scraped from the bottom of the wells and technical duplicates from each concentration were merged into a single tube. Samples were then centrifuged for 5 min at 1000×*g* to remove cellular debris and proteins. Supernatant was transferred to a conical tube and 10 mL of MeOH was added. Samples were centrifuged for 5 min at 1000×*g*, transferred to glass tubes and MeOH was evaporated under a nitrogen stream using a TurboVap system (Caliper Life Sciences, Hopkinton, MS, USA) at 40 °C until dryness. Residual dry matter was dissolved in 250 μL of MeOH.

The prepared final solutions from the assays were analyzed by liquid chromatography-mass spectrometry (LC/MS). All analyses were performed using a Waters Acquity ultra-performance liquid chromatography (UPLC, Waters Corp., Milford, Massachusetts, USA) coupled to a Q-TOF Premier quadrupole-time-of-flight mass spectrometer (QTOF-MS; Waters Corp., Milford, Massachusetts, USA) equipped with an electrospray ionization source. The UPLC system was equipped with a 1.7 μ BEH C18 column (100 × 4 mm) for chromatographic separation of MCs. The eluents A and B were acetonitrile with 0.1% formic acid (v/v) and water with 0.1% formic acid (v/v), respectively, and the flow rate was 0.4 ml/min. The sample acquisition was performed in positive ionization mode in the *m/z* range from 50 to 1100 Da. The details of the mass spectrometric settings were described elsewhere (Terzic and Ahel, 2011). For the quantitative assessment of individual MCs, the acquired full scan chromatograms were reconstructed using accurate masses of the corresponding $[M+H]^+$ ions of MCs as follows: MC-LR (m/e 995.557), MC-YR (m/e 1045.536), MC-LW (m/e 1025.535), MC-LF (m/e 986.524) and MC-LA (m/e 910.493). The representative chromatograms are given in the Supplementary Material (Fig. S1). The confirmation of peak identities as well as the quantitative assessment was performed using authentic standards as described above.

2.5. Homology modelling and molecular docking studies

Biovia Discovery Studio Client v18.1. (Dassault Systèmes, Vélizy-Villacoublay, France) implemented Build Homology Models protocol was used to construct Oatp1d1 homology model based on alignment of the model sequence and the template structure - crystal structure of the glycerol-3-phosphate transporter from *Escherichia coli* (PDB ID: 1pw4) (Yafei Huang et al., 2003). Build Homology Models protocol uses the MODELER (Sali and Blundell, 1993) automodel to build homology models. To build an Oatp1d1 homology model, the input sequence alignment between the model sequence of Oatp1d1 and the sequence of glycerol-3-phosphate transporter was obtained using the Align Sequences protocol (Sequence Identity: 11.6%, Sequence Similarity: 34, 3%). The alignment was analyzed and long insertions that could not be modeled correctly were excised from the alignment in order to obtain a reliable model. The N-terminal variable region and the large extracellular and intracellular loops/regions that were judged to be unreliable and not important for ligand binding were excised.

The remaining parameters in the Parameters Explorer of the Build Homology Models protocol were set as follows: Cut Overhangs was set to True to cut the terminal residues of the input model sequence that were not aligned with the templates; Number of Models was set to 10 to specify the number of models to create from an initial structure with Optimization Level set to High to define the proportion of molecular dynamics with simulated annealing to perform. As to building refinement models on detected loop regions, i.e., the model sequence regions of at least 5 residues length which are not aligned with the template, Refine Loops was set to True. Build Homology Models protocol uses the DOPE (Discrete Optimized Protein Energy) (Shen and Sali, 2006) method to refine loops. Refine Loops Number of Models was set to 5 to define the number of models to be created by loop optimization, and Refine Loops Optimization Level was set to Low to define the number of models to be created by loop optimization. Refine Loops with Use Discrete Optimized Protein Energy (DOPE) Method was set to High Resolution. After running Build Homology Models protocol, the Best Model Structure Superimposed to Templates was selected from the generated output models for the final three-dimensional model structure of Oatp1d1. Finally, the selected model was manually adjusted and minimized using the Smart Minimizer algorithm. The dielectric constant used to minimize the Oatp1d1 model was set to 2 corresponding to the

dielectric properties of saturated hydrocarbons as instructed when modelling a membrane system.

Microcystin congeners to be docked in the homology model of Oatp1d1 were created with ChemBio3D Ultra 13.0 (PerkinElmer, Inc., Waltham, MA, USA) and minimized using the Minimize Ligands protocol implemented in Biovia Discovery Studio Client v18.1. Flexible Docking protocol (Koska et al., 2008) was used for the molecular docking study with flexible amino acid side-chains which comprises the following steps: ChiFlex receptor conformations calculation, ligand conformations creation, LibDock docking of the ligand into active protein conformation sites, poses clustering to remove similar ligand poses, ChiRotor protein conformations rebuilding by refining selected protein side-chains in the presence of the rigid ligand, and a final CDOCKER ligand refinement. The selected homology model of Oatp1d1 was used as the rigid receptor, while the binding site within the homology models was defined by a sphere (r = 25 Å) surrounding the central pore. The rest of the parameters included in the FlexibleDocking protocol were set as follows. Maximum number of processed protein conformations was set to 100; Minimum angel, i.e. torsion angle cutoff (degrees) to determine whether the two side-chain chi1 angles are the same or not, was set to 30; Maximum number of residues for generating side chain conformations was set to 16 and these were the following: Met37, Lys38, Glu63, Ile70, Arg172, Glu176, Tyr199, Ile203, Val206, Val347, Phe350, Ile351, Ile354, Leu575, and Arg578; Conformation Method, i.e. algorithm for generating ligand conformations, was set to BEST; Maximum number of conformations to be created was set to 255; Energy Threshold, i.e. conformations of separate isomers are created inside this relative energy threshold (kcal/mol), was set to 20. LibDock ligand docking parameters inside FlexibleDocking protocol were set as follows: Number of Hotspots, i.e. number of polar or apolar receptor hotspots for conformer matching and Max Number to Save were set to 100 and 20, respectively with Tolerance for a hotspots matching algorithm for docking ligands set to 0.25; Maximum Number of Hits which defines the maximum number of hits saved for each ligand during hotspots matching prior to final pose minimization was set to 100 with Final Score Cutoff, i.e. fragment of the reported top scoring poses set to 0.5; Maximum number of poses to be kept per conformation was set to 30 with Maximum number of conformations for each ligand set to 1000; Steric Fraction specifying the number of clashes before the pose-hotspot alignment is discontinued was set to 0.10 inside the 0.5 Å Final Cluster Radius; maximum values for the Apolar SASA Cutoff and Polar SASA Cutoff were set to 15.0 Å and 5.0 Å, respectively. Lastly, a simulated annealing refinement was performed.

2.6. Statistical analysis

All studies were performed in two to three independent experiments. Data from all experiments were analyzed and related calculations done using Microsoft Office Excel 2007 and GraphPad Prism 5 for Windows for statistical analysis, respectively. Data from Oatp1d1 transport activity measurements are expressed in percentages of LY uptake. Concentration-dependent LY uptake was calculated by using equation (1):

$$I_i = ((F_i - F_m) / (F_c - F_m)) \text{ x } 100 \quad (1)$$

where I_i is the percentage of inhibition for the test concentration i, F_i is the mean fluorescent value for test concentration i, F_m is the mean fluorescent value for mock and F_c is the mean fluorescent value for control. Serial dilutions of the test compounds were log transformed and results were analyzed by non-linear regression method used for obtaining dose-response curves, with 95% confidence intervals (CI). When possible and justified with respect to the intensity of the response, IC_{50} values that designate the concentrations that cause 50% of maximal observed inhibition were calculated from sigmoidal dose-response curves using equation (2):

$$y = b + (a - b) / (1 + 10^{((LogIC50 - x) * h)}) \quad (2)$$

where y is the response, b is the minimum (bottom) of response, a represents the maximum (top) response, hillslope (h) is the slope of the curve, *LogIC50* is the halfway response from bottom to top and x is the logarithm of inhibitor concentration.

For Michaelis-Menten experiments, the obtained kinetic parameters, K_m and V_{max} values were calculated using the Michaelis–Menten equation (3),

$$V = (V_{max} \text{ x } [S]) / ([S] + K_m) \quad (3)$$

where V is the velocity (nanomoles of substrate per microgram of proteins per minute), V_{max} is the maximal velocity, [S] is the substrate concentration (micromoles) and K_m is the Michaelis-Menten constant. Data obtained were fitted using nonlinear regression analysis with GraphPad Prism.

For construction of Lineweaver-Burk plots (or double reciprocal), equation (4) was used:

$$1/V = \text{Km} / \text{Vmax} (1 / [\text{S}]) + 1 / \text{Vmax} \quad (4)$$

The plots are graphical representation of the of Oatp1d1-mediated transport kinetics, with y-axis intercept as 1/Vmax and x-axis intercept as −1/Km. The type of inhibition was determined with analysis of lines convergence. Intersecting lines that converge at the y-axis indicate the competitive inhibition modality, whereas intersecting lines that converge to the left of the y-axis and on the x-axis indicate noncompetitive inhibition modality (Copeland, 2005).

3. Results

3.1. Strength of interaction of tested MCs with zebrafish Oatp1d1 uptake transporter

In the first step of our study we tested the strength of interaction of six selected MC congeners towards the zebrafish Oatp1d1 transporter, as determined by the inhibition of uptake of model Oatp1d1 substrate Lucifer yellow (LY) in transiently transfected HEK293 FlpIn/Oatp1d1 cells. As can be seen on Fig. 1, the tested MC congeners markedly differed in their potency to inhibit LY transport. Apart from MC-RR, all other congeners significantly inhibited LY uptake in transiently transfected cells upon a short, 5 min co-exposure with LY. The most potent interactors were MC-LW and -LF that resulted in an almost complete inhibition of LY uptake in transfected cells (95 and 82%, respectively) with IC_{50} values of 0.21 and 0.26 μM, respectively. Significant inhibitory potency was also determined for MC congeners -LA, -LR and -YR, resulting in 38%, 20% and 16% inhibition of LY transport, respectively (Fig. 1).

3.2. Determining the type of interaction of tested MCs with zebrafish Oatp1d1 uptake transporter

3.2.1. Michaelis-Menten transport kinetics

All five MCs initially shown to interact with zebrafish Oatp1d1 with varying potency were further tested for their type of interaction. Our primary goal was to discern between substrates and inhibitors of zebrafish Oatp1d1, and in order to obtain more robust data and decrease variability among experiments that is often present when using transient expression protocols, related experiments were performed using HEK293 Flp-In cells stably overexpressing zebrafish Oatp1d1 (HEK293 Flip-In/Oatp1d1) instead of the transient transfection protocol used for the initial determination of the interaction strength.

Determinations of the type of interaction with zebrafish Oatp1d1 performed indirectly, using Michaelis-Menten transport kinetics experiments. Our data showed a clear pattern of K_m increase and no significant changes in V_{max} for MC congeners -LW and -LF, revealing that they

are competitive inhibitors of LY transport mediated by zebrafish Oatp1d1. Data were less conclusive for congener -LA. Although the same pattern of the K_m increase was nominally obtained, suggesting a competitive inhibition, both Michaelis-Menten kinetics (Fig. 2) and Lineweaver-Burk plots (Fig. S4) suggest rather a mixed type of inhibition. On the contrary, MC-LR and -YR appeared not to be zabrafish Oatp1d1 substrates as they rather acted as un-competitive inhibitors, showing a decrease in both K_m and V_{max} values (Table 1, Fig. 2). Yet, we have to note that in terms of statistical robustness, data for MC-LR were relatively weak, as a nominal decrease in K_m was not statistically significant with respect to data obtained for MC-LR at a 10 μm concentration. This indicates that non-competitive inhibition (characterized by no changes in K_m and decrease in V_{max}) could also have been a likely explanation.

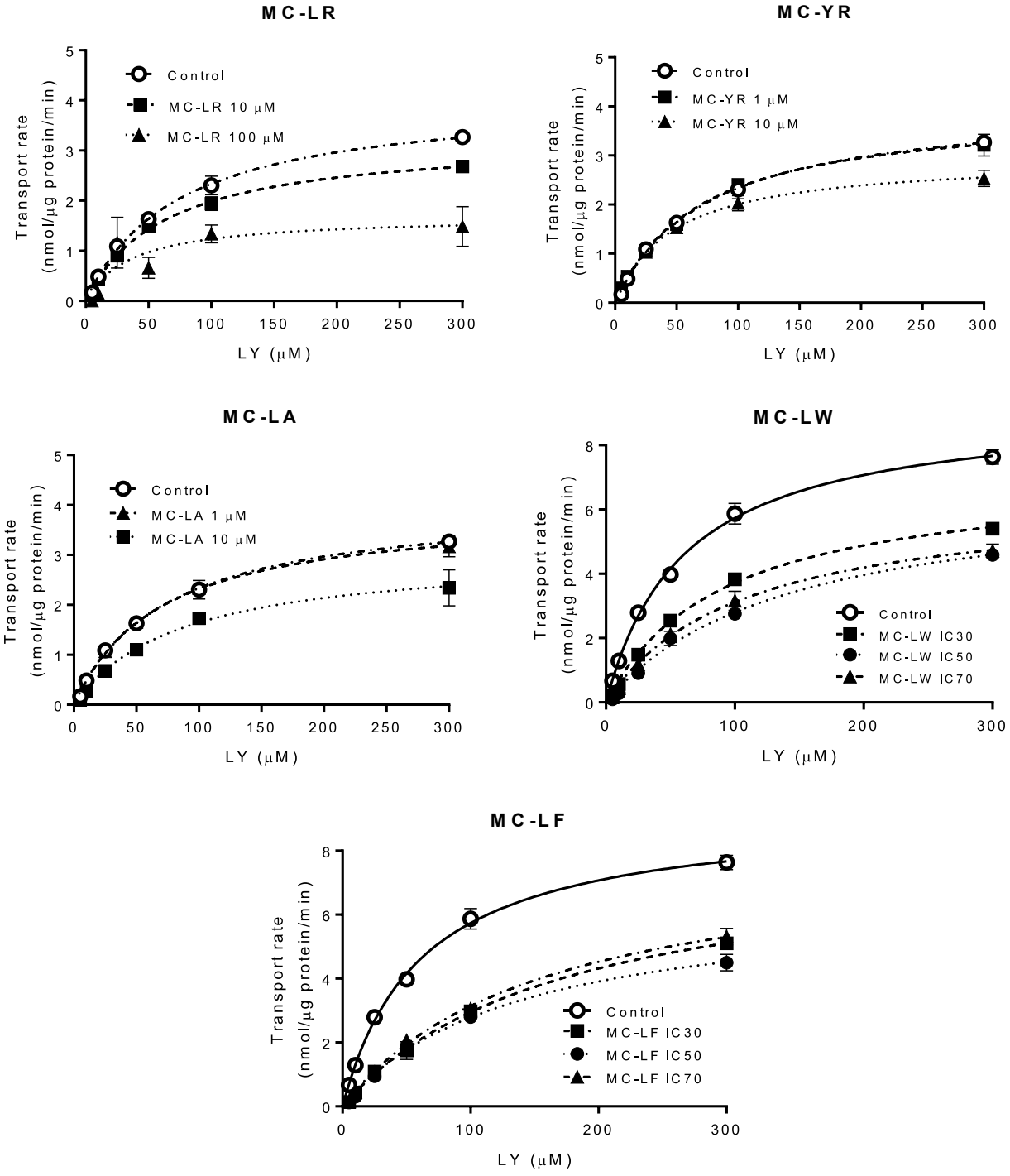

Fig. 2. Michaelis-Menten kinetics of zebrafish Oatp 1d1 mediated uptake of model fluorescent substrate LY in the presence of MC congeners -LR, -YR, LA, -LW and -LF as determined in HEK293 Flp In/Oatp1d1 overexpressing cells. The curves show concentration dependence of Oatp1d1 mediated LY uptake expressed as transport rate (nmol/μg protein/min) over LY concentration after 15 min incubation at 37 °C in the presence of increasing concentrations of tested congeners, as selected based on results of concentration response experiments (Fig. 1): 1 and 10 μM for LC-YR and -LA; 10 and 100 μM for -LR; and for -LW and -LF congeners the concentrations that resulted in 30, 50 and 70% inhibition of LY uptake, respectively, were applied. The concentration range of LY was from 5 to 300 μM. The uptake into vector transfected HEK293 cells (mock-transfected cells) was subtracted to obtain a transporter specific uptake. Each data point represents the mean ± SD from a typical experiment out of three independent determinations.

Table 1
Determination of the type of interaction of the tested MC congeners with zebrafish Oatp1d1 using Michaelis-Menten transport kinetics experiments. Kinetic analysis of LY transport by HEK 293 Flp In/Oatp1d1 over expressing cells was determined in the absence (control) or the presence of various concentrations MC congeners, as indicated. The LY uptake followed Michaelis-Menten type kinetics, and based on the data obtained MCs were classified as substrates (competitive inhibitors) or inhibitors (non- or un-competitive) according to criteria described in Materials and Methods section. Uptake was measured after 15 min incubation at 37 °C and the results represent means ± SEs from two (LW and LF) and three (LR, YR, LA) independent experiments performed in technical duplicates, respectively.

MC congener	Conc. (μM) or IC_X	K_m± SE	V_{max} ± SE	Type of interaction
LR	Ctrl	73.97 ± 5.38	4.06 ± 0.12	un-competitive inhibition
	10	63.77 ± 14.63	3.25 ± 0.09	
	100	47.07 ± 12.63	1.69 ± 0.34	
YR	Ctrl	73.97 ± 5.38	4.06 ± 0.12	un-competitive inhibition
	1	68.47 ± 5.7	3.95 ± 0.13	
	10	47.20 ± 4.25	2.95 ± 0.09	
LA	Ctrl	73.97 ± 5.38	4.06 ± 0.12	competitive/mixed inhibition
	1	69.47 ± 6.24	3.92 ± 0.14	
	10	85.24 ± 13.86	3.95 ± 0.20	
LW	Ctrl	60.88 ± 3.93	7.27 ± 0.45	Competitive inhibition
	IC_{30}	105.70 ± 10.64	7.41 ± 0.28	
	IC_{50}	111.68 ± 5.94	7.12 ± 0.19	
	IC_{70}	140.52 ± 17.78	6.75 ± 0.41	
LF	Ctrl	60.88 ± 3.93	7.27 ± 0.45	Competitive inhibition
	IC_{30}	157.8 ± 12.84	8.09 ± 0.32	
	IC_{50}	172.8 ± 16.32	8.04 ± 0.38	
	IC_{70}	135.4 ± 13.57	7.55 ± 0.31	

3.2.2. Chemical analytical verification

The type of interaction of the tested MC congeners with zebrafish Oatp1d1 was further verified by chemical analytical determinations of the rate of accumulation of congeners upon exposure of mock-transfected and Oatp1d1 transfected cells to increasing concentrations of the tested congeners. The result of the LC/MS analyses for the highest concentration of MCs are shown in Fig. 3, while the detailed documentation of the experiments, including all concentration levels of MCs tested, can be found in Supplementary Material (Fig. S2). The results showed significant, multi-fold increases in accumulation of MC-LA, -LF, and -LW in transfected in comparison to mock-transfected cells, confirming them as substances transported by zebrafish Oatp1d1 (Figs. 3 and 4). On the contrary, no significant Oatp1d1 mediated uptake of MC-YR was observed, confirming results of Michaelis-Menten kinetics experiments and showing that MC-YR is not a zebrafish Oatp1d1 substrate. However, in contrast to data obtained by Michaelis-Menten determinations, our accumulation experiments and subsequent LC-MS analysis of MC-LR showed that this congener is actually transported by Oatp1d1, although at a comparatively low rate (Figs. 3 and 4). This suggests that MC-LR might be an Oatp1d1 substrate as well, but its transport is comparatively slow.

3.3. Homology modelling and molecular docking studies

A structure-based sequence alignment of Oatp1d1 and glycerol-3-phosphate transporter template from *E. coli* illustrating the unmodeled extracellular and intracellular portions (underlined) is shown in the Supplementary Material (Fig. S3). Good quality alignment of the model sequence and the template structure of the glycerol-3-phosphate transporter in the transmembrane regions suggested that the constructed Oatp1d1 homology model should be of reasonable quality for these regions and central pore description. The resulting homology model of Oatp1d1 is shown in Fig. 5. Model complexes of structural model of Oatp1d1 and MCs of interest were generated using flexible molecular docking where selected residues were allowed to rotate during procedure and the binding sphere (r = 25 Å) was defined large enough to encompass the majority of the central pore.

However, prior to the docking study of MCs, to validate the receptor molecule, i.e. Oatp1d1 homology model, a docking of the known model substrate LY was attempted. The successful docking predicted that LY is buried deep in the central pore approximately at its center (Fig. 6AB). The five MCs that showed significant interaction with zebrafish Oatp1d1, MC-LF and MC-LW were successfully docked without any translation of the binding site. The resulting model complexes are shown in Fig. 6C–F together with the non-bonding interactions of docked MCs

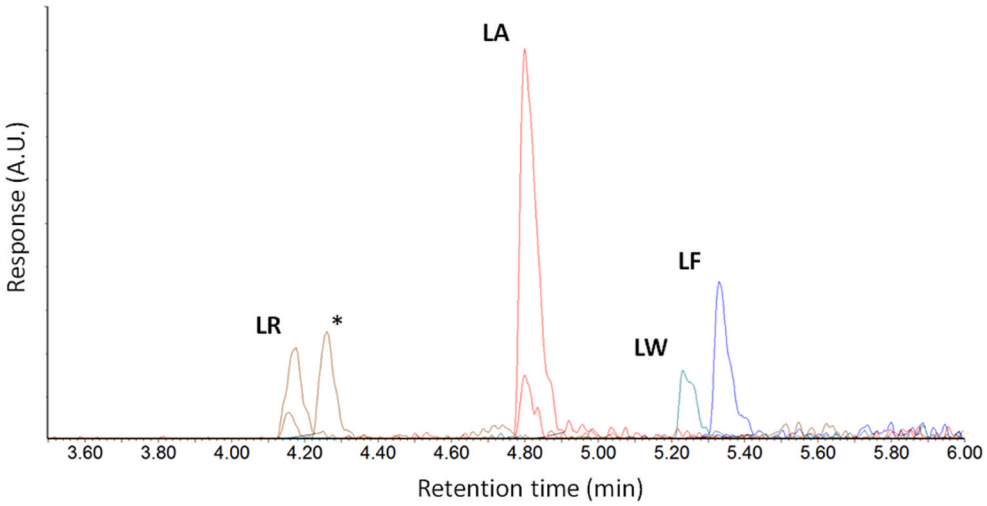

Fig. 3. Overlayed LC/MS chromatograms of Oatp1d1 uptake determinations with four selected microcystins. The traces of individual MC congeners are given in different colors as follows: MC-LR – brown, retention time (RT) 4.18 min; -LA – red, RT 4.8 min; -LW – green, RT 5.24 min; -LF – blue, RT 5.33 min; *unknown impurity (RT 4.26 min). The upper and lower traces represent responses obtained in Oatp1 transfected and mock-transfected cells, respectively. (For interpretation of the references to color in this figure legend, the reader is referred to the Web version of this article.)

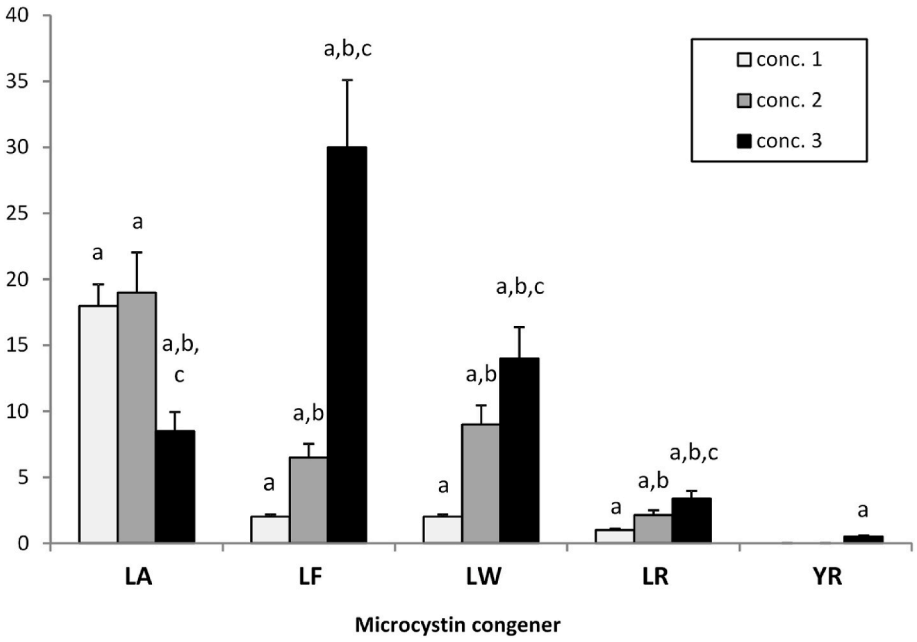

Fig. 4. Comparison of the uptake of the tested MC congeners in Oatp1d1 transfected over mock-transfected HEK293T cells. The cells were exposed to three increasing concentrations of MC congeners (0.1, 0.5 and 1 μM for MC-LW and -LF; 0.5, 1 and 5 μM for MC-LA and -YR; 5, 20 and 50 μM for MC-LR) for 30 min and the amount of accumulated MCs determined using LC-MS analysis, as described in the Materials and Methods section. Data from a typical experiment are shown as means ± SDs from triplicate determinations and represent a fold increase in the accumulation of MC congeners over the accumulation determined in mock-transfected cells for each of the three tested concentrations. One-way ANOVA and Tukey's multiple comparison test were used for determination of statistically significant differences between the uptake of corresponding MC congeners in transfected over mock-transfected cells, as well as among the uptake determined in the cells exposed to different concentrations of the same MC congener: a – significantly different ($p < 0.05$) from accumulation in mock-transfected cells; b – significantly different ($p < 0.05$) from concentration 1 of the same MC congener; c – significantly different ($p < 0.05$) from concentration 2.

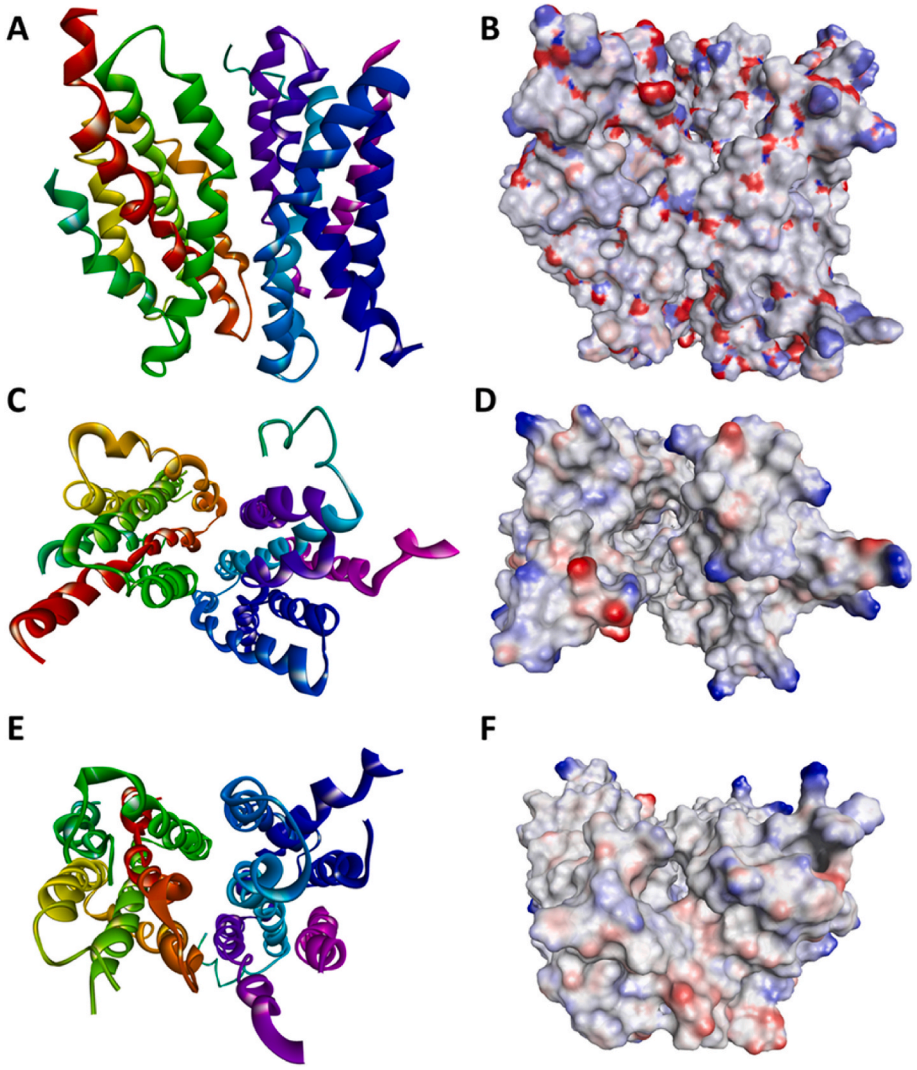

Fig. 5. Solid ribbon and rainbow-colored representation of the homology model of Oatp1d1 as viewed from the lateral side (A), the extracellular side (C) and the intracellular side (E) with electrostatic potential mapped onto its molecular surface, respectively (B, D, F). Regions of negative, positive and neutral potential are shown in red, blue and white/gray, respectively. The model is deposited and available at ModelArchive base (https://www.modelarchive.org/doi/10.5452/ma-4kkal). (For interpretation of the references to color in this figure legend, the reader is referred to the Web version of this article.)

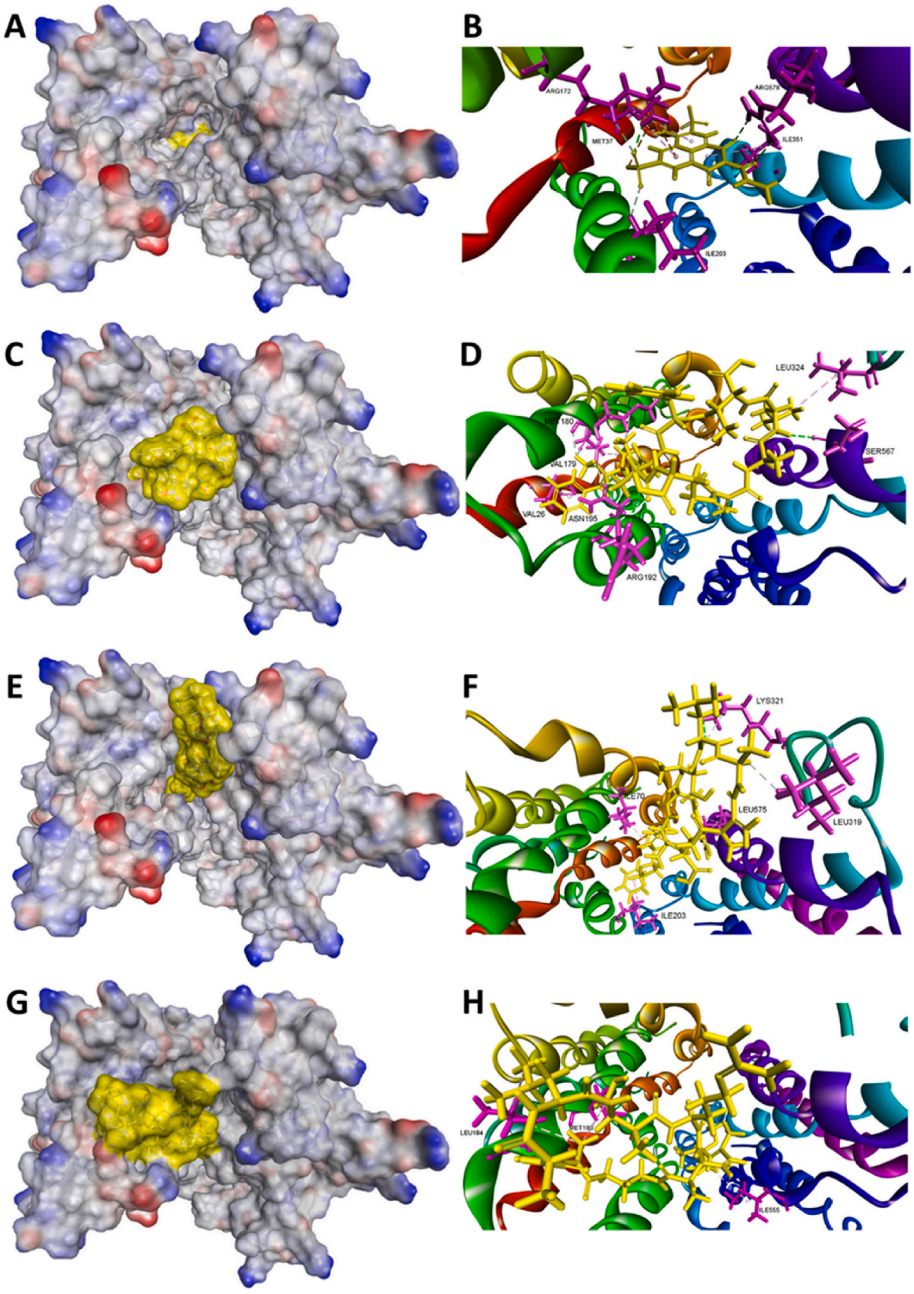

Fig. 6. Electrostatic potential mapped on the molecular surface of model complexes between structural model of Oatp1d1 and LY (A), MC-LF (C), MC-LW (E), or MC-LR (G). Regions of negative, positive and neutral potential are shown in red, blue and white/gray, respectively. The molecular surface of ligands is shown in yellow. The close-up of LY (B), MC-LF (D), MC-LW (F), or MC-LR (H) docked into the central pore of the structural model of zebrafish Oatp1d1. The ligands are shown in yellow sticks and amino acid residues engaged in non-bonding interactions (dotted lines) are shown in magenta sticks. (For interpretation of the references to color in this figure legend, the reader is referred to the Web version of this article.)

with neighboring amino acid residues. MC-LF was predicted to be placed above the center of the pore interacting non-covalently with neighboring residues identified as Ser567, Val179, Met180, Arg192, Asn195, Leu324 and Ser567. On the other hand, MC-LW was placed on the outer part of the sphere/central pore and exposed to the surrounding fluid. In doing so, MC-LW was engaged in non-bonding interactions with the following residues: Ile70, Ile203, Lys319, Lys321, and Leu575. However, the other congeners failed to fully accommodate inside the defined binding sphere without significant translation of the binding site sphere's center closer to the opening of the central pore. After the refinement of the model, the initially failed MC congeners -LA and -LR were successfully docked. The model complex between Oatp1d1 structural model and MC-LR depicts the blocking of the central pore unit by MC-LR (Fig. 6GH). The binding position of MC-LR was secured through non-bonding interactions with residues Met180, Leu184, and Ile55.

4. Discussion

Based on the studies published so far, the uptake kinetics of various MC congeners is a factor that largely determines their bioavailability and toxic potential in exposed aquatic organisms, and Oatp transporters appeared to be major contributors relevant for the uptake of MCs in fish species (Meier-Abt et al., 2007; Bury et al., 1998; Bieczynski et al., 2014; Faltermann et al., 2016; Steiner et al., 2015). Yet, more detailed studies performed recently utilizing zebrafish as a cyprinid fish model showed that the rate of MC uptake significantly varies for different congeners. Furthermore, it has been shown that zebrafish Oatp1d1 acts as a ubiquitously expressed, multi-specific transporters of various MC congeners, while other MC transporting Oatps, like members of the Oatp1f subfamily, are expressed exclusively in the kidney and transport only specific MC congeners (Steiner et al., 2015). As the primary cause for this variability could be related to the strength and type of interaction (substrates versus inhibitors) of MC congeners with fish Oatp1d1

transporter, it is logical to assume that these features may contribute to differences in the toxic potential of individual congeners towards fish species as one of the primary targets of cyanotoxins and subsequent toxic effects related to HABs. Therefore, it is highly relevant to better characterize the MC congeners frequently found in HABs with respect to their interaction with Oatp1d1. To do so, we selected six MC congeners that differ in terms of various structural properties and their log P_{OW} values (Table S1) and utilized HEK293T cells transiently or stably expressing zebrafish Oatp1d1 as a specific and sensitive assay system for testing their interaction with this transporter.

In the first part of our study, we determined the strength of interaction of the tested MCs and found that most of them do interact with zebrafish Oatp1d1, inhibiting the uptake of model Oatp1d1 substrate LY in transfected cells with varying potency. What was immediately obvious was that the strongest interactors were also the most lipophilic congeners -LW and -LF (Fig. 1), followed by congeners -LA, -LR and -YR, again in apparent correlation with their log P_{OW}. Furthermore, as the only truly hydrophilic congener, with log P_{OW} value of −0.2, MC-RR did not significantly interfere with LY transport by Oatp1d1. These results were similar to data reported earlier by Steiner et al. (2015), with the exception of MC-RR that was shown to be transported by zebrafish Oatp1d1, albeit at a slow rate and as the result of a prolonged 24 h exposure.

However, our initial data on the interaction strength, although specific enough due to the use of Oatp1d1 overexpressing cells, could not reveal if the tested MC congeners are substances transported by the zebrafish Oatp1d1 transporter, or they inhibit LY transport due to an un- or non-competitive mode of inhibition. To get a better insight into the type of interaction, in the next step of our study we performed Michaelis-Menten kinetics determinations of the type of interaction for five MC congeners shown to be Oatp1d1 interactors. Although Michaelis-Menten kinetics measurements are not a direct determination of substrate transport, we utilized it as an established experimental protocol to discern between substrates and inhibitors and showed that MC-LW and -LF clearly behaved as substrates (i.e. competitive inhibitors), while congeners -LR and -YR appeared not to be transported by Oatp1d1. (Table 1, Figs. 2 and S4). Considering the robustness of the data in respect to the calculated K_m and V_{max} values for LY transport, and their shifts in comparison to control values determined without addition of the tested MC congeners, the data obtained using this method appeared to be a good indication of congeners that are substrates versus those that act as Oatp1d1 inhibitors. The exceptions were MC-LA that were less conclusive and showed a mixed inhibiton pattern, and MC-LR where in terms of statistical robustness the data were relatively weak, as a nominal decrease in K_m was not statistically significant with respect to data obtained for MC-LR at 10 μm concentration (Table 1, Figs. 2 and S4). This indicates that non-competitive inhibition (characterized by no changes in K_m and a decrease in Vmax) could also have been a likely explanation.

In addition to Michaelis-Menten kinetics data, the transport of selected MCs by zebrafish was further studied by direct chemical analytical determination of their accumulation rate in transfected and mock-transfected cells by LC-MS analysis. The obtained results were rather consistent with the results of kinetics determinations: significant increases in accumulation of MC-LF, -LW, and -LA were determined in transfected over mock-transfected cells at all of the three concentrations of MCs, confirming them as substrates for zebrafish Oatp1d1 (Figs. 3, 4 and S2). Likewise, exposure to MC-YR did not result in a significant fold-increase in accumulation over mock-transfected cells, showing that MC-YR was not transported by Oatp1d1. Yet, two irregularities were shown. The first is related to the lack of consistent dose response for MC-LA, where the exposure of the cells to the highest concentration actually resulted in lower accumulation of MC-LA in comparison to the two lower concentrations (Fig. 4). A likely explanation for this discrepancy might be related to suboptimal range of the concentrations used. For example, although MCs interact with cellular PPs primarily by non-covalent, two-step mechanism involving rapid binding and inactivation of PPs, the process is followed by a slower (within hours) covalent interaction (Craig et al., 1996; Hastie et al., 2005; Pereira et al., 2011). However, although a shorter, 30 min methanol extraction protocol was used in our study, it is possible that a more significant covalent interaction happened at the highest MC-LA concentration used, partly preventing extraction of accumulated MC-LA by methanol. Nevertheless, even at that concentration the accumulation of MC-LA was clearly much higher in transfected over mock-transfected cells showing basically that -LA congener is also a substrate transported by zebrafish Oatp1d1.

Second inconsistency was related to MC-LR data. In contrast to partially inconclusive Michaelis-Menten analysis of MC-LR kinetics, chemical analytical determinations showed that MC-LR was transported into Oatp1d1 overexpressing cells, although at a lower rate (Figs. 3, 4, S2 and S4). These data are actually in agreement with previous reports that showed that MC-LR is an Oatp1d1 substrate in zebrafish (Steiner et al., 2015; Faltermann et al., 2016). In terms of LC-LR toxicokinetics, the detailed study by Steiner et al. (2015) is particularly relevant, as it showed that intracellular transport of MC-LR by Oatp1d1 is much less favorable when compared to transport of more hydrophobic congeners like -LW or -LF, which are transported much faster. Consequently, although the authors correctly pointed out that kinetic values obtained in various studies using different exposure regimes, model substrates and/or detection methods should not be directly compared, we believe the overall pattern determined in our study is quite consistent with previous reports, which indicates that MC-LR is a slow, low affinity substrate for Oatp1d1 transporter.

Finally, to confirm experimentally observed different modes of action among the tested compounds, a structural study was undertaken utilizing molecular modelling. Since a crystal structure of zebrafish Oatp1d1 is not available, a homology model was constructed based on a chosen template crystal structure of the glycerol-3-phosphate transporter from *E. coli* solved in a conformation with the central pore opening toward the intracellular side (Meier-Abt et al., 2006; Yafei Huang et al., 2003). Although the used template structure was not ideal in terms of the sequence similarity (Fig. S3), and long insertions that could not be modeled correctly were excised from the alignment in order to obtain a reliable model, all of the excised insertions were either from the N-terminal region or large extracellular/intracellular loops/regions not important for ligand binding. As a result, the final alignment of the model sequence and the template structure was of substantial quality, implying that the Oatp1d1 homology model constructed (Fig. 5) could be used for reliable molecular docking studies. It was further confirmed by successful docking of LY as a verified substrate for zebrafish Oatp1d1, which was docked deep in the central pore of zebrafish Oatp1d1 (Fig. 6AB). Moreover, LY was predicted to interact with Met37 via a hydrophobic π-alkyl non-covalent bond, and this residue corresponds to the position of Arg45 in the model glycerol-3-phosphate transporter described as one of the key residues for substrate binding, located at the closed end of the substrate-translocation pathway in the middle of the membrane (Yafei Huang et al., 2003).

As to the docking studies of MC congeners, although all five MCs were studied and the most potent interactors MC-LF and MC-LW were successfully docked, others initially failed to fully accommodate inside the defined binding sphere. Such an outcome could have been expected for MC-YR, which was shown both indirectly (Michaelis-Menten knetics) and directly (chemical analytical determinations) not to be transported by zebrafish Oatp1d1, but the docking of MC-LA and -LR inside the Oatp1d1 central pore, however, was expected. Nevertheless, after the refinement of the model by translation of the binding site sphere's center closer to the opening of the central pore, MC-LA and -LR were successfully docked. Interestingly, it can be seen that MC-LR is placed higher above the central pore when compared with the predicted binding pose of MC-LF, and bulky MC-LR is clearly prevented from easily entering the central pore.

Furthermore, although no crystal structures of the OATPs/Oatps are

available and the transport mechanism of OATPs/Oatps has not been fully elucidated, the available *in silico* models imply that transport of their substrates most probably occur through a central, positively charged pore (Meier-Abt et al., 2005a, 2005b). Consequently, as Oatps are primarily anion transporters, the presence of positively charged arginine residues in MC-LR, -YR, and -RR probably contributed to its lower affinities towards zebrafish Oatp1d1. Considering the strength and type of interaction of tested MCs versus their physicochemical descriptors, our data support earlier observations (Karlgren et al., 2012; Wolman et al., 2013) which indicated that apart from lipophilicity, properties like topological polar surface area and hydrogen bond features correlate with the potency of various substances, including MCs (Table S1), for interaction with OATPs/Oatps, including zebrafish Oatp1d1.

5. Conclusion

Taken together, the data obtained in this study support results by similar studies implying that the zebrafish Oatp1d1 is a membrane transporter that could be a rate limiting step for the uptake of microcystins in cyprininds, and possibly other teleosts. However, although a wide substrate preference and a rather large binding region of zebrafish Oatp1d1 do enable the transport of structurally and chemically different MC congeners, it seems to be highly plausible that the transport of MCs could be largely dependent on their basic physicochemical properties, with log P_{OW} being the most obvious determinant.

Secondly, as previously suggested by Steiner et al. (2015), the presence of nominally highly toxic MC congeners (e.g., MC-LR) in cyanobacterial blooms does not necessarily translate to high ecological risk if their capacity for Oatp1d1 transport is low. And vice versa, the presence of nominally less toxic MCs (e.g., MC-LF or -LA) that are in contrast readily taken up by Oatp1d1 can result in highly relevant deleterious effects in exposed fish, especially neurotoxicity and renal toxicity in organs and tissues characterized by significant expression of Oatp1d1 or related transporters with overlapping substrate specificities.

Consequently, apart from the determination of chemical composition of HABs in relation to MCs, a reliable risk assessment should take into account the interaction of identified MC congeners with Oatp1d1 as their primary transporter in fish species. As demonstrated, the use of highly specific *in vitro* models in combination with uptake and kinetics determinations, chemical analytical verification and *in silico* molecular docking studies could be used as a reliable experimental setup for this goal.

Declaration of competing interest

The authors declare that they have no known competing financial interests or personal relationships that could have appeared to influence the work reported in this paper.

Acknowledgements

This research was financed by the Croatian Science Foundation (Project No. IP-2019-04-1147) and partially supported under the STIM-REI project, Contract Number: KK.01.1.1.01.0003, a project funded by the European Union through the European Regional Development Fund – the Operational Programme Competitiveness and Cohesion 2014–2020 (KK.01.1.1.01). The computational resources and Biovia Discovery Studio Client v18.1 software (Dassault Systèmes, Vélizy-Villacoublay, France), used for homology modelling and molecular docking studies, were provided through Croatian Science Foundation projects (grant numbers HrZZ-IP-2013-11-4307 and HrZZ-IP-2018-01-7683).

Appendix A. Supplementary data

Supplementary data to this article can be found online at https://doi.org/10.1016/j.chemosphere.2021.131155.

Author contributions

PM – designed and performed majority of interaction and exposure experiments related to chemical analytical determinations, and wrote the manuscript; MA – LC-MS determinations; NM – homology modelling and molecular docking studies; JL and IM – performed part of Michaelis-Menten kinetics studies; TS – supervision of the project, study conception and design, writing of the paper with input from all authors.

References

Bieczynski, F., De Anna, J.S., Pirez, M., Brena, B.M., Villanueva, S.S.M., Luquet, C.M., 2014. Cellular transport of microcystin-LR in rainbow trout (*Oncorhynchus mykiss*) across the intestinal wall: possible involvement of multidrug resistance-associated proteins. Aquat. Toxicol. 154, 97–106.

Bouaïcha, N., Miles, C.O., Beach, D.G., et al., 2019. Structural diversity, characterization and toxicology of microcystins. Toxins 11, 714.

Bradford, M., 1976. A rapid and sensitive method for the quantification of microgram quantities of protein utilizing the principle of protein-dye binding. Anal. Biochem. 72, 248–254.

Buratti, F.M., Manganelli, M., Vichi, S., Stefanelli, M., Scardala, S., Testai, E., Funari, E., 2017. Cyanotoxins: producing organisms, occurrence, toxicity, mechanism of action and human health toxicological risk evaluation. Arch. Toxicol. 1, 1049–1130.

Bury, N.R., Newlands, A.D., Eddy, F.B., Codd, G.A., 1998. *In vivo* and *in vitro* intestinal transport of 3H-microcystin-LR, a cyanobacterial toxin, in rainbow trout (*Oncorhynchus mykiss*). Aquat. Toxicol. 42, 139–148.

Chen, J., Xie, P., Li, L., Xu, J., 2009. First identification of the hepatotoxic microcystins in the serum of a chronically exposed human population together with indication of hepatocellular damage. Toxicol. Sci. 108, 81–89.

Copeland, R.A., 2005. Evaluation of enzyme inhibitors in drug Discovery. In: Journal of Chemical Information and Modeling. A John Wiley & Sons, Inc., Hoboken, New Jersey https://doi.org/10.1017/CBO9781107415324.004.

Craig, M., Luu, H.A., McCready, T.L., Holmes, C.F.B., Williams, D., Andersen, R.J., 1996. Molecular mechanisms underlying the interaction of motuporin and microcystins with type-1 and type-2A protein phosphatases. Biochem. Cell. Biol. 74, 569–578, 1996.

Dittmann, E., Fewer, D.P., Neilan, B.A., 2013. Cyanobacterial toxins: biosynthetic routes and evolutionary roots. FEMS Microbiol. Rev. 37, 23–43.

D'Anglada, L.V., Hilborn, E.D., Backer, L.C. (Eds.), 2016. Harmful Algal Blooms (HABs) and Public Health: Progress and Current Challenges. Toxins special edition (MDPI Books).

Faltermann, S., Prétôt, R., Pernthaler, J., Fent, K., 2016. Comparative effects of nodularin and microcystin-LR in zebrafish: 1. Uptake by organic anion transporting polypeptide Oatp1d1 (Slco1d1). Aquat. Toxicol. 171, 69–76.

Ferrão-Filho Ada, S., Kozlowsky-Suzuki, B., 2011. Cyanotoxins: bioaccumulation and effects on aquatic animals. Mar. Drugs 9, 2729–2772.

Fischer, W.J., Altheimer, S., Cattori, V., Meier, P.J., Dietrich, D.R., Hagenbuch, B., 2005. Organic anion transporting polypeptides expressed in liver and brain mediate uptake of microcystin. Toxicol. Appl. Pharmacol. 203, 257–263.

Fischer, A., Hoeger, S.J., Stemmer, K., Feurstein, D.J., Knobeloch, D., Nussler, A., Dietrich, D.R., 2010. The role of organic anion transporting polypeptides (OATPs/SLCOs) in the toxicity of different microcystin congeners *in vitro*: a comparison of primary human hepatocytes and OATP-transfected HEK293 cells. Toxicol. Appl. Pharmacol. 245, 9–20.

Hagenbuch, B., Meier, P.J., 2003. The superfamily of organic anion transporting polypeptides. Biochim. Biophys. Acta Biomembr. 1609, 1–18.

Hastie, C., Borthwick, E., Morrison, L., Codd, G., Cohen, P., 2005. Inhibition of several protein phosphatases by a non-covalently interacting microcystin and a novel cyanobacterial peptide, nostocyclin. BBA Gen 1726, 187–193.

Karlgren, M., Vildhede, A., Norinder, U., Wisniewski, J.R., Kimoto, E., Lai, Y., Haglund, U., Artursson, P., 2012. Classification of inhibitors of hepatic organic anion transporting polypeptides (OATPs): influence of protein expression on drug–drug interactions. J. Med. Chem. 55, 4740–4763.

Komatsu, M., Furukawa, T., Ikeda, R., Takumi, S., Nong, Q., Aoyama, K., Akiyama, S., Keppler, D., Takeuchi, T., 2007. Involvement of mitogen-activated protein kinase signaling pathways in microcystin-LR-induced apoptosis after its selective uptake mediated by OATP1B1 and OATP1B3. Toxicol. Sci. 97, 407–416.

Koska, J., Spassov, V.Z., Maynard, A.J., Yan, L., Austin, N., Flook, P.K., Venkatachalam, C.M., 2008. Fully automated molecular mechanics based induced fit protein-ligand docking method. J. Chem. Inf. Model. 48, 1965–1973.

Lončar, J., Smital, T., 2018. Interaction of environmental contaminants with zebrafish (*Danio rerio*) multidrug and toxin extrusion protein 7 (Mate7/Slc47a7). Aquat. Toxicol. 205, 193–203.

MacKintosh, C., Beattie, K.A., Klumpp, S., Cohen, P., Codd, G.A., 1990. Cyanobacterial microcystin-LR is a potent and specific inhibitor of protein phosphatases 1 and 2A from both mammals and higher plants. FEBS Lett. 264, 187–192.

Marić, P., Ahel, M., Senta, I., Terzić, S., Mikac, I., Žuljević, A., Smital, T., 2017. Effect-directed analysis reveals inhibition of zebrafish uptake transporter Oatp1d1 by caulerpenyne, a major secondary metabolite from the invasive marine alga *Caulerpa taxifolia*. Chemosphere 174, 643–654.

McLellan, N.L., Manderville, R.A., 2017. Toxic mechanisms of microcystins in mammals. Toxicol. Res. (Camb) 6, 391–405.
Meier-Abt, F., Mokrab, Y., Mizuguchi, K., 2005a. Organic anion transporting polypeptides of the OATP/SLCO superfamily: identification of new members in nonmammalian species, comparative modeling and a potential transport mode. J. Membr. Biol. 208, 213–227.
Meier-Abt, F., Mokrab, Y., Mizuguchi, K., 2005b. Organic anion transporting polypeptides of the OATP/SLCO superfamily: identification of new members in nonmammalian species, comparative modeling and a potential transport mode. J. Membr. Biol. 208, 213–227.
Meier-Abt, F., Hammann-Hänni, A., Stieger, B., Ballatori, N., Boyer, J.L., 2007. The organic anion transport polypeptide 1d1 (Oatp1d1) mediates hepatocellular uptake of phalloidin and microcystin into skate liver. Toxicol. Appl. Pharmacol. 218, 274–279.
Niedermeyer, T.H.J., Daily, A., Swiatecka-Hagenbruch, M., Moscow, J.A., 2014. Selectivity and potency of microcystin congeners against OATP1B1 and OATP1B3 expressing cancer cells. PloS One 9, e91476.
Pereira, S.R., Vasconcelos, V.M., Antunes, A., 2011. The phosphoprotein phosphatase family of Ser/Thr phosphatases as principal targets of naturally occurring toxins. Crit. Rev. Toxicol. 41, 83–110.
Popovic, M., Zaja, R., Smital, T., 2010. Organic anion transporting polypeptides (OATP) in zebrafish (*Danio rerio*): phylogenetic analysis and tissue distribution. Comp. Biochem. Physiol. Mol. Integr. Physiol. 155, 327–335.
Popovic, M., Zaja, R., Fent, K., Smital, T., 2013. Molecular characterization of zebrafish Oatp1d1 (Slco1d1), a novel Organic anion transporting polypeptide. J. Biol. Chem. 288, 33894–33911.
Sali, A., Blundell, T.L., 1993. Comparative protein modelling by satisfaction of spatial restraints. J. Mol. Biol. 234, 779–815.
Shen, M.Y., Sali, A., 2006. Statistical potential for assessment and prediction of protein structures. Protein Sci. 15, 2507–2524.
Sivonen, K., Jones, G., 1999. Cyanobacterial toxins. In: Chorus, I., Bartram, J. (Eds.), Toxic Cyanobacteria in Water: A Guide to Public Health Significance, Monitoring and Management. E&FN Spon, London, pp. 41–111.
Steiner, K., Zimmermann, L., Hagenbuch, B., Dietrich, D., 2015. Zebrafish Oatp-mediated transport of microcystin congeners. Arch. Toxicol. 90, 1129–1139.
Terzic, S., Ahel, M., 2011. Nontarget analysis of polar contaminants in freshwater sediments influenced by pharmaceutical industry using ultra-high-pressure liquid chromatography-quadrupole time-of-flight mass spectrometry. Environ. Pollut. 159, 555–566.
Wang, H., Xu, C., Liu, Y., Jeppesen, E., Svenning, J.C., Wu, J., Zhang, W., Zhou, T., Wang, P., Nangombe, S., Ma, J., Duan, H., Fang, J., Xie, P., 2021. From unusual suspect to serial killer: cyanotoxins boosted by climate change may jeopardize megafauna. Innovation 2 (2), 100092.
Wolman, A.T., Gionfriddo, M.R., Heindel, G.A., Mukhija, P., Witkowski, S., Bommareddy, A., VanWert, A.L., 2013. Organic anion transporter 3 interacts selectively with lipophilic β-lactam antibiotics. Drg. Metabol. Disp. 41, 791–800.
Yafei Huang, M., Lemieux, J., Song, J., Auer, M., Da-Neng, W., 2003. Structure and mechanism of the glycerol-3-phosphate transporter from *Escherichia coli*. Science 301, 616–620.
Zohdi, E., Abbaspour, M., 2019. Harmful algal blooms (red tide): a review of causes, impacts and approaches to monitoring and prediction. Int. J. Environ. Sci. Technol. 16, 1789–1806.